Oil Slick Characterization Using an Airborne Laser Fluorosensor- Construction Considerrations

Andersson, P. S; Montan, Sune; Svanberg, Sune

1985

Oil Slick Characterization Using an Airborne Laser Fluorosensor

-

Construction Considerations

P. Stefan Andersson, Sune Montán and Sune Svanberg

Lund Reports on Atomic Physics

LRAP-45

July 1985

Oil Slick Characterization Using an Airborne Laser Fluorosensor - Construction Considerations

P. Stefan Andersson, Sune Montán and Sune Svanberg

Department of Physics, Lund Institute of Technology, P. O. Box 118, S - 221 00 Lund, Sweden

Abstract

Experiments aiming at the assessment of suitable parameters for an airborne laser fluorosensor have been performed. Particular emphasis is put on the possibilities to characterize an oil spill by overflying a slick, first detected e.g. by a side-looking airborne radar (SLAR) system. A practical system suitable for a small aircraft is proposed.

1. Introduction

Oil spills from tankers, deliberate or accidental, constitute a major threat to coastal regions, and efficient detection systems allowing a launching of adequate counter measures are of great interest. Oil slick detection can be based on different physical principles, such as differences in the reflection of microwaves or IR radiation, or on the monitoring of fluorescence following laser excitation. A side-looking airborne radar (SLAR) system operating on cm waves constitutes a particularly powerful, all-weather imaging detection system. Such a system is based on the reduction in the sea clutter in the microwave scattering because of the smoothing of the surface capillary waves that normally are present on the sea surface when the wind speed exceeds 10 m/s. However, while a spill is effectively localized using such a system little information on the nature of the oil is obtained. Laser-induced fluorescence (LIF) yields such information by analyzing the spectral distribution of the emitted light.

The present report concentrates on the possibilities to use a simple laser fluorosensor for characterizing oil-spills that have

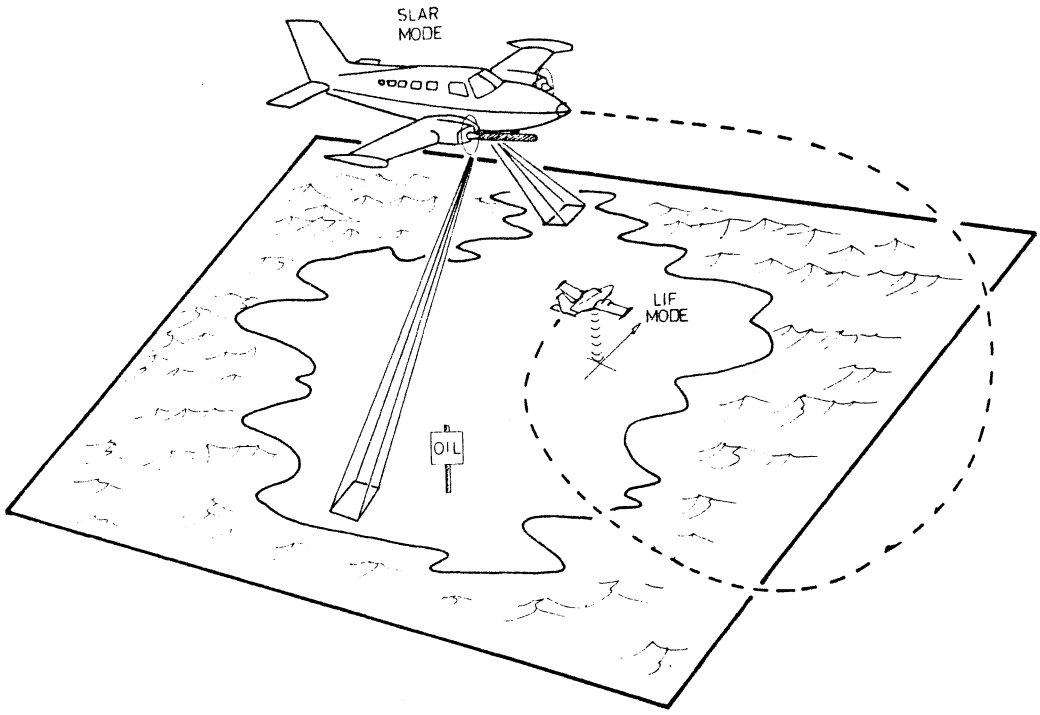

Fig. 1. SLAR detection and LIF characerization of a marine oil spill.

already been detected by a SLAR system as outlined in Fig. 1. Especially, we consider the possibility to supplement the Swedish Maritime Surveillance System, developed by the Swedish Space Corporation, with such a unit. The existing system incorporates an Ericsson SLAR system and an optional Ericsson IR scanning radiometer. Both units provide images of the sea surface showing areas covered by oil. The IR system yields some information on the oil layer thickness. None of the instruments gives any information on the oil type. Thus, a laser fluorosensor would be very valuable if it could provide the lacking information leading to a possibility to decide what action responsible authorities should take to minimize damage and cost. Since the surveillance system is intended for small aircrafts, size and weight of a LIF system are important considerations.

Considerable research and development work concerning airborne maritime LIF monitoring has been performed by many groups since 1970. These efforts include theoretical calculations, laboratory

measurements and flight tests. Some of the material on remote LIF oil detection and characterization can be found in Refs.[1-15]. The suppression of the water OH-stretch Raman emission because of the oil absorption has also been efficiently utilized to detect and quantify oil spills. By studying asymmetries in the water Raman band from uncovered water, temperature can be assessed, since the fractions of mono-, di- and polymer water vary with temperature [16,17,18]. Closely related to oil studies are investigations aiming at studies of pelagic algae observing the 685 nm chlorophyll LIF peak [19-28]. Airborne lasers can also be used for non-spectroscopic applications such as laser bathymetry [29-33] using the blue-green transmission window of water. Our group has also been involved in prior activities in the laser marine probing field. Our studies include determinations of LIF signatures for oils and other chemicals, algae and fish [34-39]. Bathymetric tank experiments have also been performed [40]. LIF as well as bathymetric tests have been performed in coastal Swedish waters in a ship-based field test [41].

In considering airborne LIF measurements for characterizing oil slicks many aspects have to be taken into account. The question whether it is possible to distinguish between different types of oil using their spectral LIF signatures must be answered. Further, the strength and signature of the oil fluorescence in comparison to the fluorescence from water, algae and "Gelbstoff" is another important point. It is highly desirable to be able to operate a fluorosensor also during daytime, and therefore the influence of the background light in the detection of the visible LIF is of paramount importance. Since the background radiation level B is largely independent of the object distance r, while the LIF signal is reduced with an $1/r^2$ dependance, the possible operating height will be strongly influenced by the level of background radiation and, of course, also by the available laser power P. Clearly, it is advantageous to operate with a low beam divergence, since the receiving telescope field-of-view can then be reduced accordingly with a corresponding reduction in the background signal. What has just been said can be expressed in a formula for the received signal S:

$$S = C * P * \Phi^2 * f(\delta) * F(\lambda) / r^2 \qquad (1.1)$$

Here, $f(\delta)$ is a function of the oil layer thickness δ. For low δ values $f(\delta)$ increases linearly with δ to finally reach a saturated value f_{sat}, which is obtained for "optically thick" layers. $F(\lambda)$ represents the spectral response of the detection system (photomultiplier and optical filters). C is a system constant and Φ is the telescope diameter. The signal should be compared with the background signal B, which can be expressed as

$$B = I_s(T) * \Delta t * \Omega * \Phi^2 * F(\lambda) \qquad (1.2)$$

where $I_s(T)$ is the surface radiance that strongly varies with the time T of the day/night. B is reduced by keeping the solid angle of observation Ω low and by using a short gate time Δt in the detection system. However, it should be noted that Δt must be sufficiently large so that signal is not lost because of small variations in the flight height r. Clearly the surface echo occurring at a time delay of $2r/c$ after the transmission of the laser pulse, c being the velocity of light, must fall inside the gate window Δt.

In the next section we will first describe laboratory measurements of fluorescence spectra for oil and water samples.Then experiments in which the fluorescence from remote samples was detected using transient digitizing techniques in a LIDAR set-up with filter-selected spectral bands are presented. This is followed by an account of remote measurements on a water barrel using full spectral resolution. In Section 3 we will discuss the results and draw conclusions from our measurements. In a final section a prototype airborne fluorosensor is proposed, that under specified conditions would provide the spectral information that would complete the measuring capabilities of an airborne maritime surveillance system.

2. Measurements

2.1. Laboratory measurements

In preparation for subsequent measurements, spectra of relevant oil and water samples were captured in the laboratory using the set-up shown in Fig. 2. A EG&G PAR optical multi-channel analyzer Model 1215 with a Model 1420 detector in the focal plane of a Jarrell-Ash Monospec 18 spectrograph was used. The light source here, as well as in the other measurements performed, was a nitrogen laser which emitted 3-5 ns pulses at 337 nm with a maximum repetition rate of 20 Hz. The elastically scattered laser light was suppressed by means of a Schott WG 360 cut-off filter in front of the entrance slit of the spectrograph. As an intensity standard a specified layer thickness of a 70 µg/ℓ solution of Rhodamine 6 G in water was used. The fluorescence intensity of this standard at its peak wavelength defines the intensity unit. In Figs. 3a and 3b the spectra of some relevant

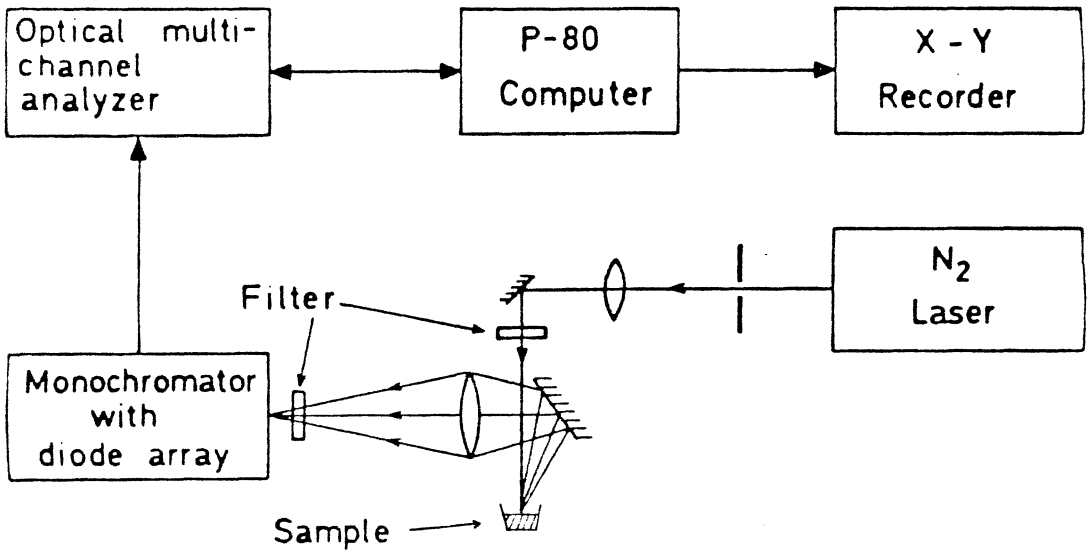

Fig. 2. Laboratory set-up for spectral studies of laser-induced fluorescence.

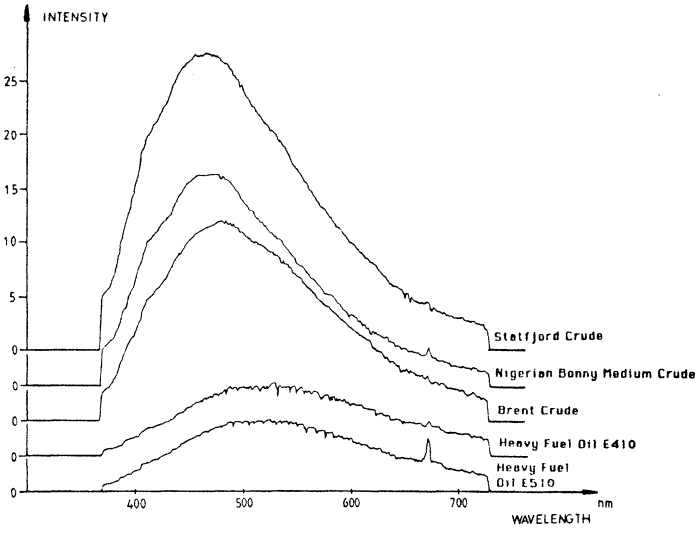

Fig. 3a. Spectra of different crude oils and refined products. The intensity unit is the peak fluorescence of a 3 mm thick layer of a 70 µg/ℓ Rhodamine solution in water.

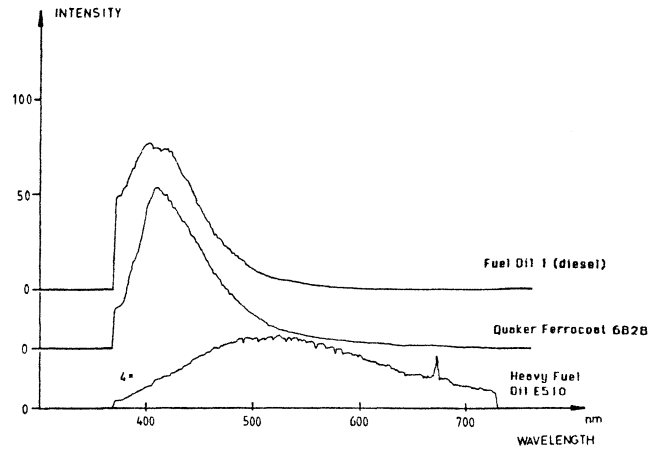

Fig. 3b. Spectra of oil products. The spectrum of the Heavy Fuel Oil E510 is drawn to a four times enlarged scale.

oils are shown. It can be seen that oils of the same type exhibit similar fluorescence while the different types differ considerably from each other. This is in accordance with the results in Ref. [34] in which a large number of oil fluorescence spectra have been examined. The peak at 674 nm is the laser light reflected in the second order by the spectrograph grating. In Fig. 4a and b some different water spectra are shown. The peak at 384 nm is the Raman peak due to the OH stretch vibration at 3400 cm^{-1}. All spectra have been corrected for the varying spectral response of the detection system. To distinguish the oil type the intensity at three different wavelengths, A at 410 nm, B at 465 nm and C at 525 nm can be measured and the ratios A/B and B/C formed. A crude oil would then give A/B < 1 and B/C > 1, a heavy fuel oil A/B < 1 and B/C < 1 and a refined product A/B > 1 and B/C > 1. The intensities at these wavelengths and the ratios are tabulated in Table 1 The reason for comparing wavelength intensities by

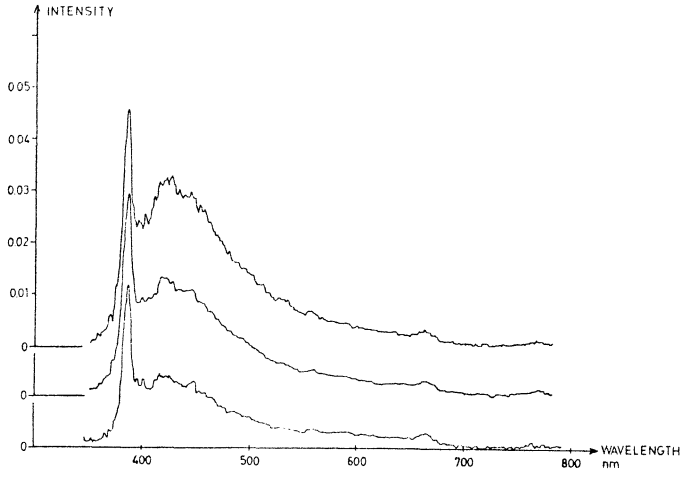

Fig. 4a. Spectra of some North sea water samples.

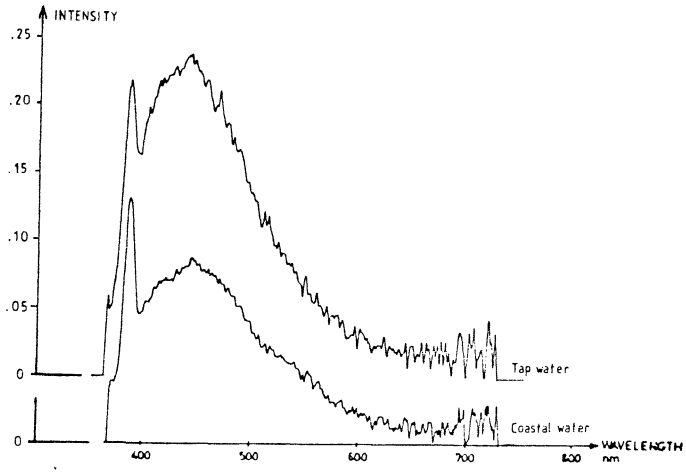

Fig. 4b. Spectra of tap water and coastal water.

forming ratios is, as pointed out in Ref. [42], that a dimensionless ratio is insensitive to target distance changes, laser power fluctuations and target topography variations.

	INTENSITY AT			RATIOS	
	A 410 nm	B 465 nm	C 525 nm	A/B	B/C
STATFJORD CRUDE	19	27	21	0.70	1.3
NIGERIAN BONNY MEDIUM CRUDE	12	19	14	0.63	1.4
BRENT CRUDE	11	18	16	0.61	1.1
HEAVY FUEL OIL E410	2.5	5.3	6.6	0.47	0.80
HEAVY FUEL OIL E510	2.5	5.6	6.6	0.45	0.85
FUEL OIL 1 (DIESEL)	75	29	4.3	2.6	6.7
QUAKER FERRO-COAT 6828	85	39	10	2.2	3.9
NORTH SEA WATER	0.001	0.00085	0.00045	1.2	1.9

Table 1. Intensities at different wavelengths for the oils in Figs. 3 and the water in Fig. 4a and some relevant intensity ratios.

2.2. Range measurements

Range measurements were performed outdoors through an open window. A range overview is shown in Fig. 5. The oil was placed in a tub on the roof of a building about 70 m away and the beam was deflected down into the tub by a mirror. An optically thick oil sample was placed in the tub, either on the bottom or on top of a water layer as indicated in the figure. A surface monitoring

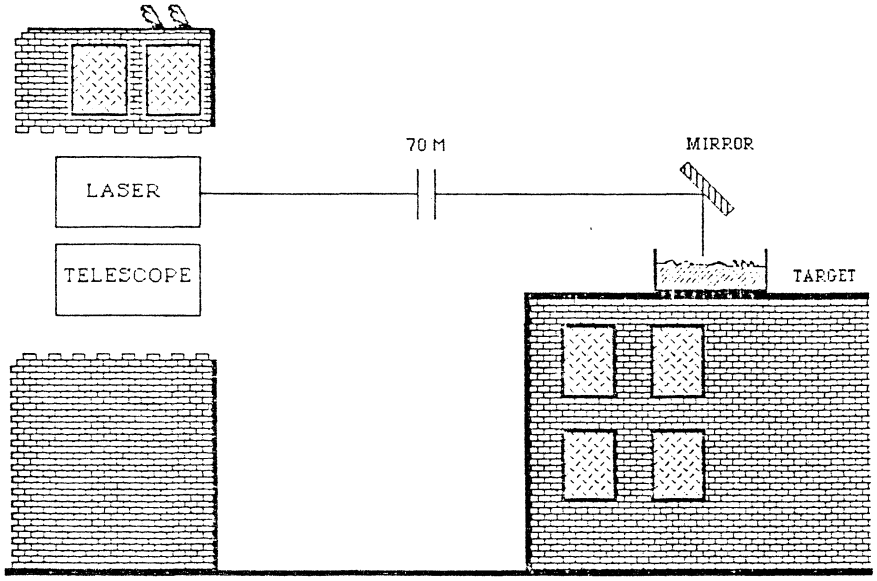

Fig. 5. Overview of range measurements set-up.

system that was constructed at the department and described in Ref. [38] was used. A lay-out of the system is shown in Fig. 6. The nitrogen laser was a PRA Model LN 250 emitting 5 ns pulses with 250 μJ of energy. To get a low beam divergence the laser light was passed through beam-shaping lenses. Due to reflection and transmission losses the pulse energy out from the system was reduced to about 100 μJ. Two different telescopes were used, a ϕ=15 cm lens telescope as shown in Fig. 6 and a Newton telescope with 25 cm diameter. For the detection, a photomultiplier tube (PMT) for each telescope was used. In front of the PMT's bandpass filters were placed. Measurements were performed at three different wavelengths in the violet, green and orange region. The PMT signals were recorded either by a transient digitizer (Biomation model 8100) having a 10 ns resolution, or by the gated integrators (500 ns gate width) in the surface monitoring system (Evans Associates, Model 4130) as shown in Fig. 7.

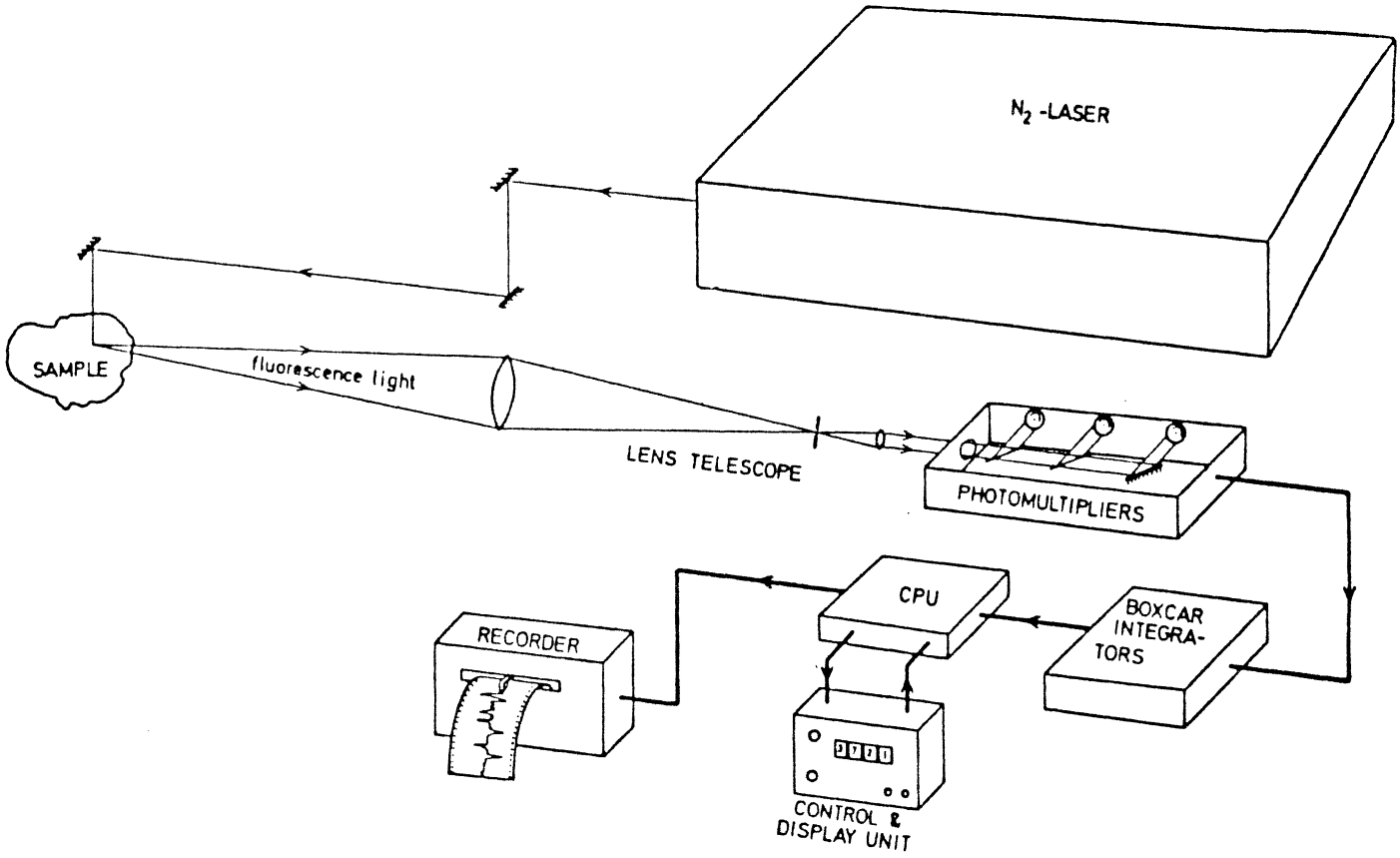

Fig. 6. The surface monitoring system used for the gated integrator recordings.

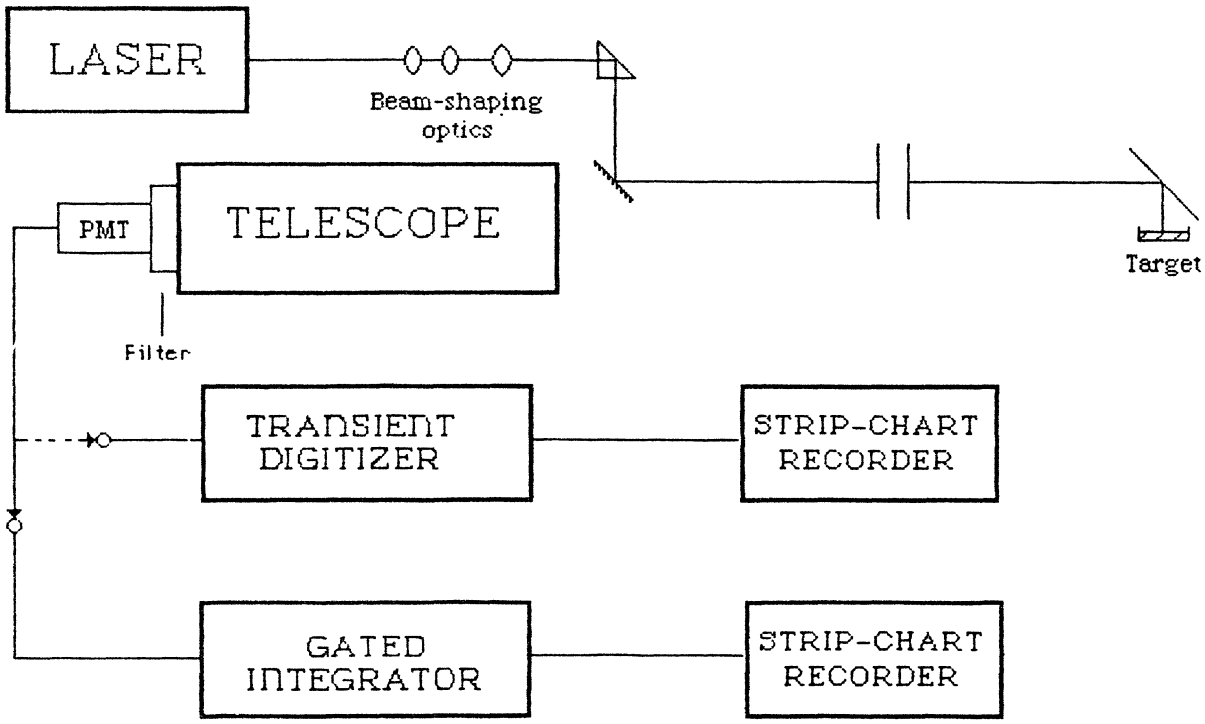

Fig. 7. Laboratory set-up for range mesurements.

Figs. 8-10 show different recordings from these set-ups. In Figs. 8 and 9 the target consisted of Quaker Ferrocoat 6828 rust-protective oil (spectrum in Fig. 3b). Fig. 8 shows transient

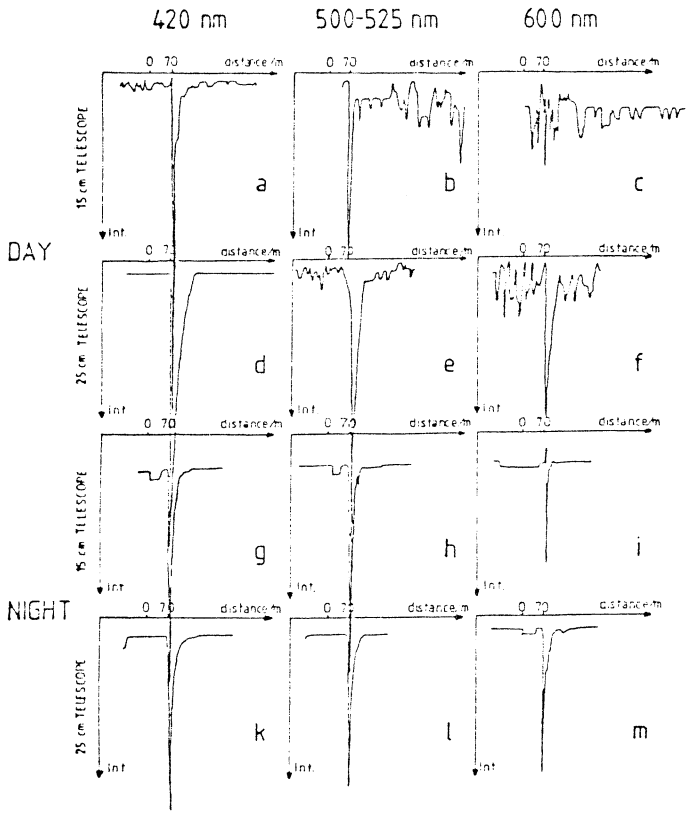

Fig. 8. Recordings from single shots made with a transient digitizer showing signal, noise and background levels for different combinations of telescope, ambient light conditions and wavelengths. The green light measured was for the Φ = 15 cm telescope at 500 nm and for the Φ = 25 cm telescope at 525 nm.

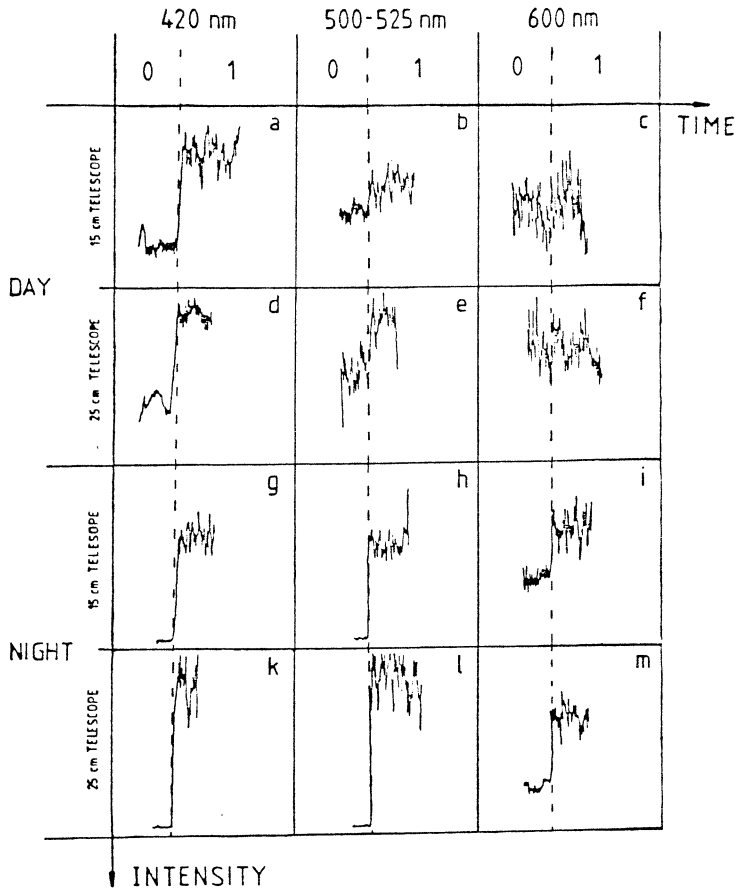

Fig. 9. Recordings made using the gated integrator showing signal, noise and background levels for the same signals as in Fig. 8. The gate width was 500 ns. The green light measured was as in Fig. 8.

digitizer traces from single shots recorded at different wavelengths with two different telescopes under different ambient light conditions. In Fig. 9 a recording of the same signals with the gated integrators is shown. It is clear from the figures that the ambient light level is very important for the detection limits. The 600 nm signals are evident with both the detection systems at night-time but they get completely buried in the background when daylight is present. The gate width is important

		TRANSIENT DIGITIZER			GATED INTEGRATORS		
		420 nm	500/525 nm	600 nm	420 nm	500/525 nm	600 nm
DAY	SMALL TELESCOPE	30	3	<1	.2	<1	<1
	LARGE TELESCOPE	>50	11	3	5	1.5	<1
NIGHT	SMALL TELESCOPE	>50	>50	35	4	4	1.5
	LARGE TELESCOPE	>50	>50	35	3	3	2

Table 2. S/N-ratios for different detection combinations.

for background light suppression. A shorter gate time would make the signals in Figs. 8b and 8e stand out more palpable than actually obtained in Figs. 9b and 9e. The difference in spectral response of the photomultipliers used, S-4 for the small telescope and S-20 for the big one is seen in Figs. 9i and 9m. S-20 has about five times the response of S-4 at 600 nm. The recordings in Figs. 9g-9m appear quite noisy despite the absence of background in Figs. 8g-8m. This is photon noise due to the limited number of photons reaching the telescope. The pulse-to-pulse variations are not seen in the tran-

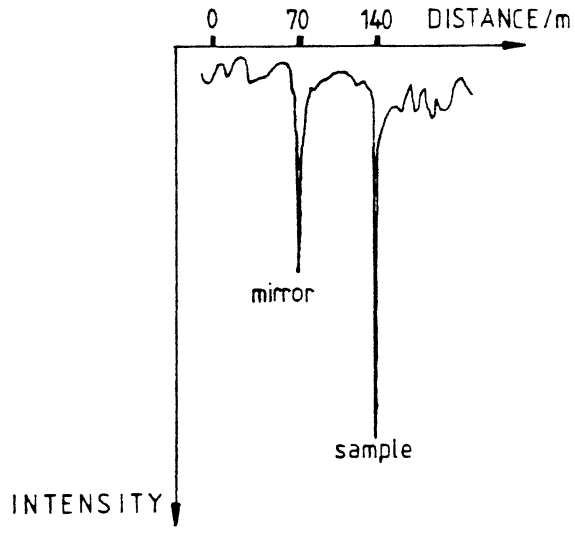

Fig. 10. Folded-path LIF. The mirror was adjusted so that the laser beam hit the target 140 m away.

sient digitizer recordings since these cover single shots only. The S/N ratios for these measurements are evaluated in Table 2.In Fig. 10 a folded path recording made with the transient digitizer is shown. In this case the mirror in Fig. 5 was arranged so that the laser beam was reflected back towards the window adjacent to the set-up and there the target was placed. Thus, the target distance was 140 m. The target consisted of a normal piece of bleached paper, which fluoresces even more intensely than the Ferrocoat 6828 oil. The fluorescence of the mirror contaminations is seen at 70 m distance.

The day measurements in Figs. 8-10 were all performed under cloudy weather conditions. In bright sunshine the background light problem of course increases. This is demonstrated in Fig. 11. Fig. 11 contains a recording of signal and background levels at 420 nm obtained at different laser pulse energies. Here, a tripled Nd:YAG laser at 355 nm was used as a light source in connection with the gated integrator detection system with 500 ns gate and the 15 cm telescope. The distance was 70 m and the

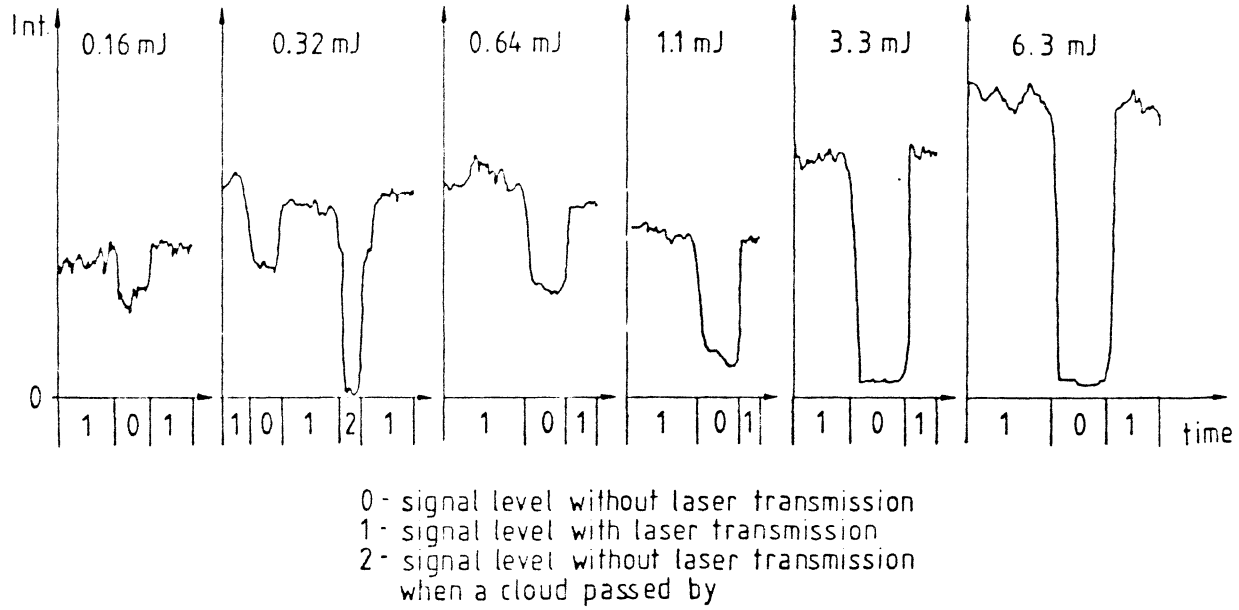

Fig. 11. Gated integrator recordings of the 420 nm fluorescence of the Quaker Ferrocoat 6828 oil, induced by different laser pulse energies from a 355 nm Nd:YAG-laser. The magnifications are different for the curves, which means that only the S/N ratios are significant for a comparison between the curves.

target was again the 6828 oil. The recording was performed on a bright sunny April day. In the second recording in Fig. 11 a cloud passed by, however, and as can be seen the background level difference between cloudy and sunny light conditions is evident. As a matter of fact, it can be seen that the oil fluorescence signal level is only about 1/3 of the sunshine background signal. It is also seen in the figure that under these circumstances a pulse energy of a least 0.3 mJ is required to get an acceptable signal-to-noise ratio.

2.3 Measurements in water

As a comparison to the oil fluorescence studied in the previous sections, now also water fluorescence will be investigated. In order to get a maximum, and for this purpose relevant, water fluorescence signal, an optically thick column of water has to be exposed. For an oil the thickness of an optically thick layer is of the order of μm but for water it is of the order of m. Therefore, with the aim to get the integrated fluorescence from deep water, a 2 meter high water barrel was constructed. The inside of the barrel was made of aluminum for preventing the barrel itself from fluorescing under the N_2-laser excitation.

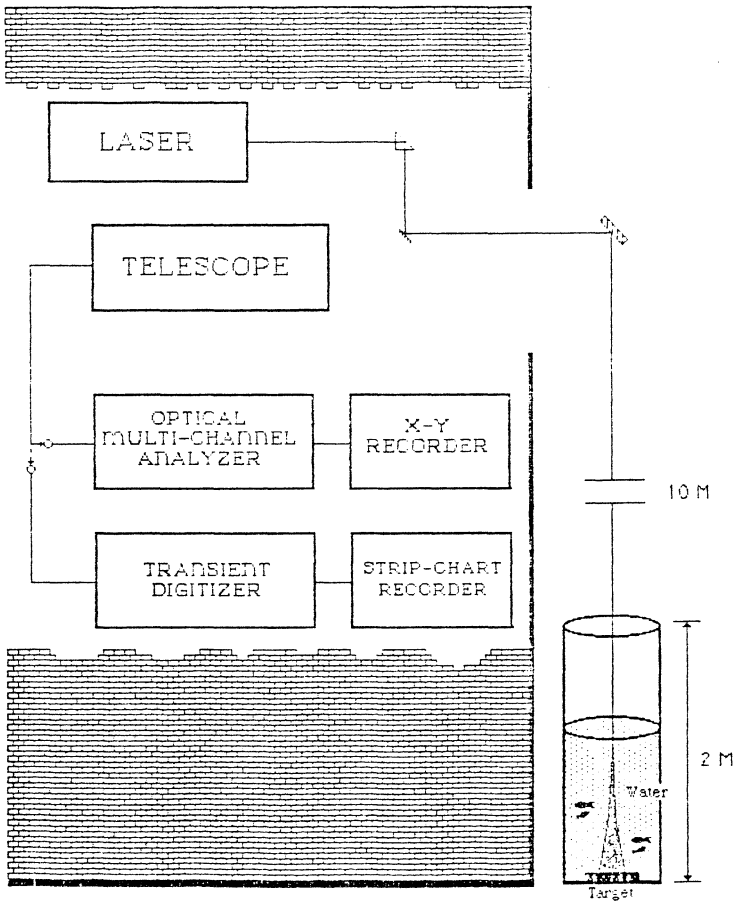

Fig. 12. Laboratory set-up for measurements involving water.

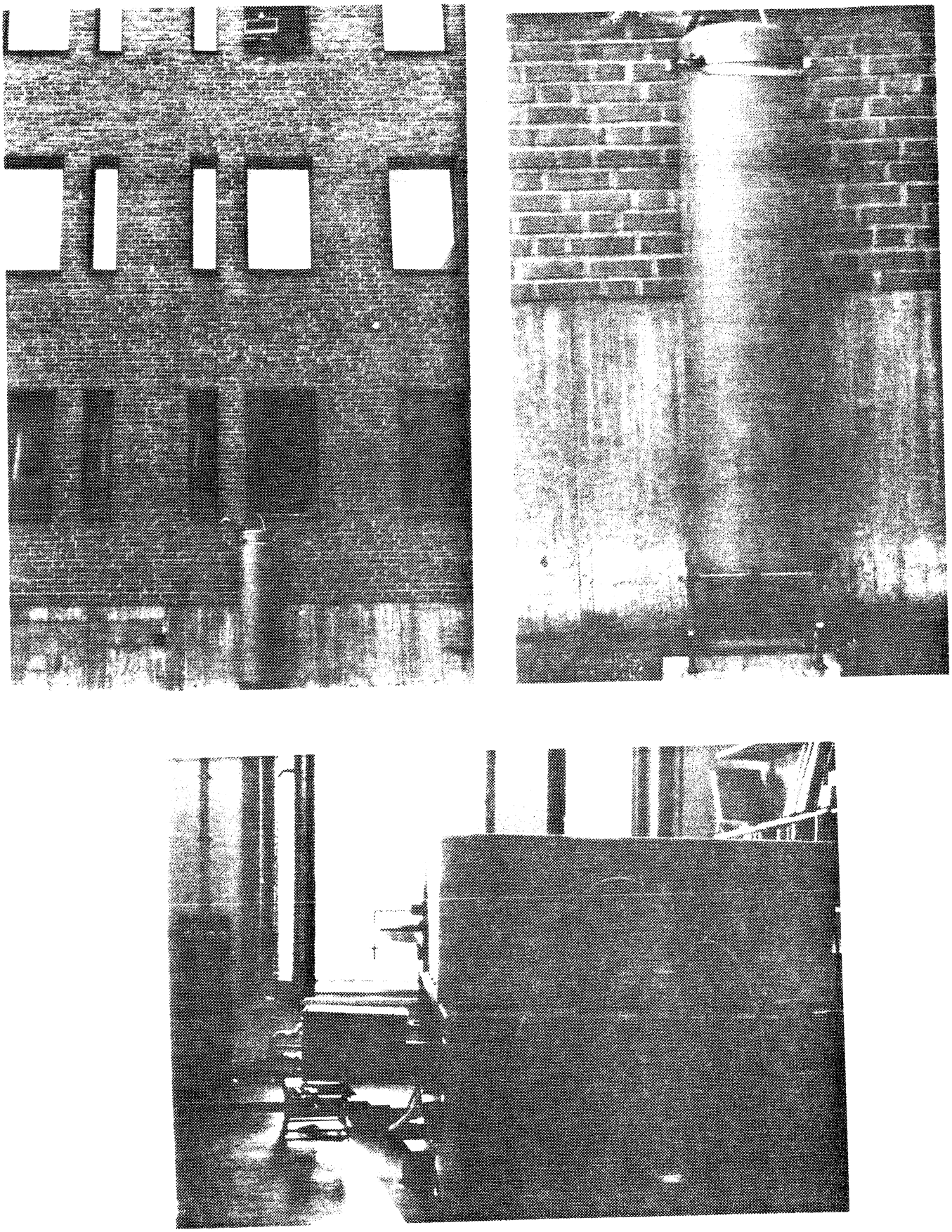

Fig. 13. Photographs of the barrel and the set-up used for the measurements with water. The size of the barrel was h = 1.80 m and Φ = 0.5 m.

Both kinds of setups described in Sections 2.1 and 2.2 were used for these experiments. Thus, in one part of the measurements the optical multi-channel analyzer from 2.1 was placed behind the collecting 15 cm telescope. The set-up is shown in Figs. 12 and 13. A strong signal had to be present to capture the total spectral information from the fluorescence at this distance. In particular this was needed in a measurement performed to make clear to what water depth it was possible to detect a target with our equipment. For this purpose we used a plastic sheet, that had a strong fluorescence centered at about λ=410 nm when illuminated with the N_2-laser. This sheet was placed on the bottom of the barrel, which slowly was filled up with water. (All measurements were performed with tap water. A comparison between tap water and sea water is done below). For each 10 cm water depth increment a spectrum was acquired. Some of these recordings are presented in Fig. 14. The penetrating laser intensity

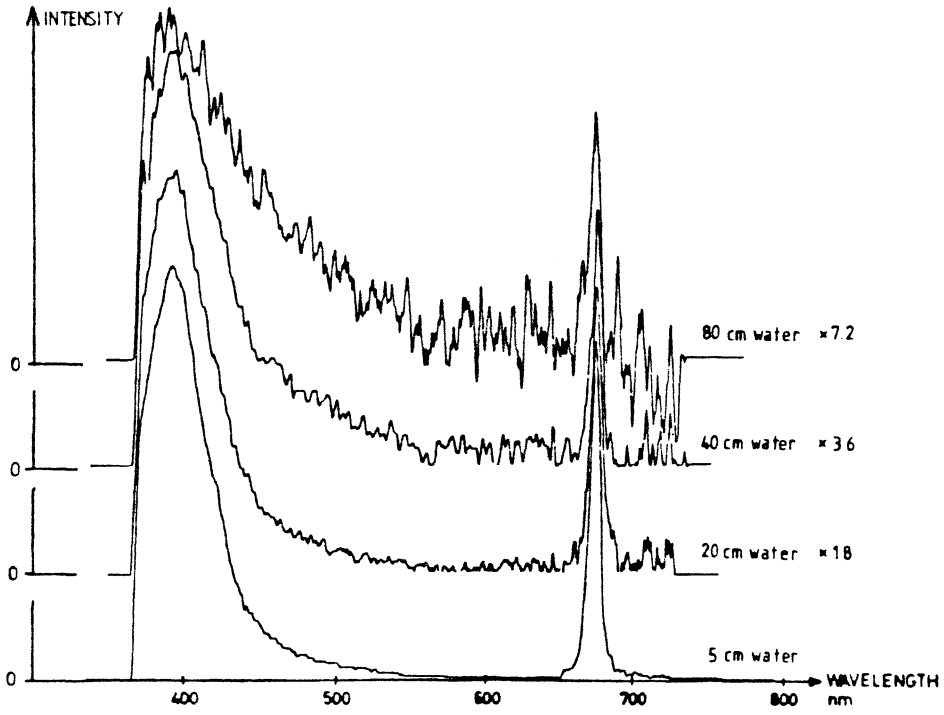

Fig. 14. Spectra of a plastic sheet in water for different water depths. The plastic fluorescence peak is centered around λ = 410 nm and the peak at 674 nm is the reflected laser light in the second grating order.

should decrease according to Beer-Lambert's law as $I=I_0e^{-\alpha x}$, where α is the absorption coefficient for water at the laser wavelength used and x is the actual penetration depth. The plastic fluorescence measured at a specific wavelength should therefore be

$$I_p(d) = I_0(1-R_1)^2 q_p e^{-(\alpha+\beta)d} \qquad (2.3.1)$$

β is here the absorption coefficient in water for the detection wavelength, d is the water depth, q_p is the plastic quantum yield and R_1 is the reflection in the air-water surface.

In the experiments, however, the measured quantity is the plastic fluorescence with the water fluorescence added. The water fluorescence will be integrated with the depth. If we neglect the reflection in the plastic sheet, limit the problem to a first order approximation and assume that a constant fraction q_w (the water quantum yield) of the absorbed laser energy will cause fluorescence into the right solid angle, the fluorescence intensity from the water will be

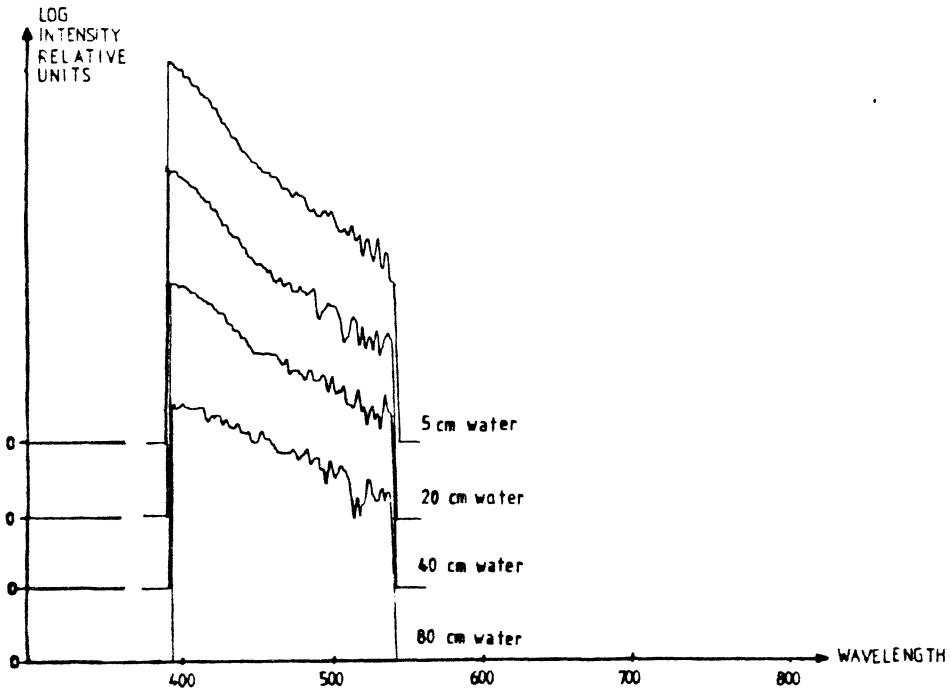

Fig. 15a. A logarithmic representation of part of the curves in Fig. 14. Observe that the curves have shifted place compared to Fig. 14.

$$I_w(d) = I_0(1-R_1)^2 \int_0^d q_w e^{-(\alpha+\beta)x} dx = I_0(1-R_1)^2 q_w \frac{1 - e^{-(\alpha+\beta)d}}{\alpha+\beta} \quad (2.3.2)$$

Now, the plastic fluorescence is much stronger than the specific water fluorescence, which therefore should not influence the measurements in shallow water. Only when most of the laser intensity is absorbed in the water it should affect the fluorescence spectrum. The peak fluorescence intensity should therefore approximately decrease linearly for small depths in a logarithmic plot. This is also shown in Figs. 14 and 15. Fig. 14 shows the attenuation of both the laser and the fluorescence light. They are not equal but the laser wavelength is more suppressed than the 410 nm fluorescence in water. It can also be seen that the water fluorescence at about 440 nm is growing with the depth. Figs. 15 a and b show that the natural logarithm of the measured intensity decreases almost linearly with the depth for small water depths. For deeper water the water fluorescence is no more negligible and affects the total measured intensity. It will of course saturate on the level for infinity deep water when d has increased beyond a certain depth.

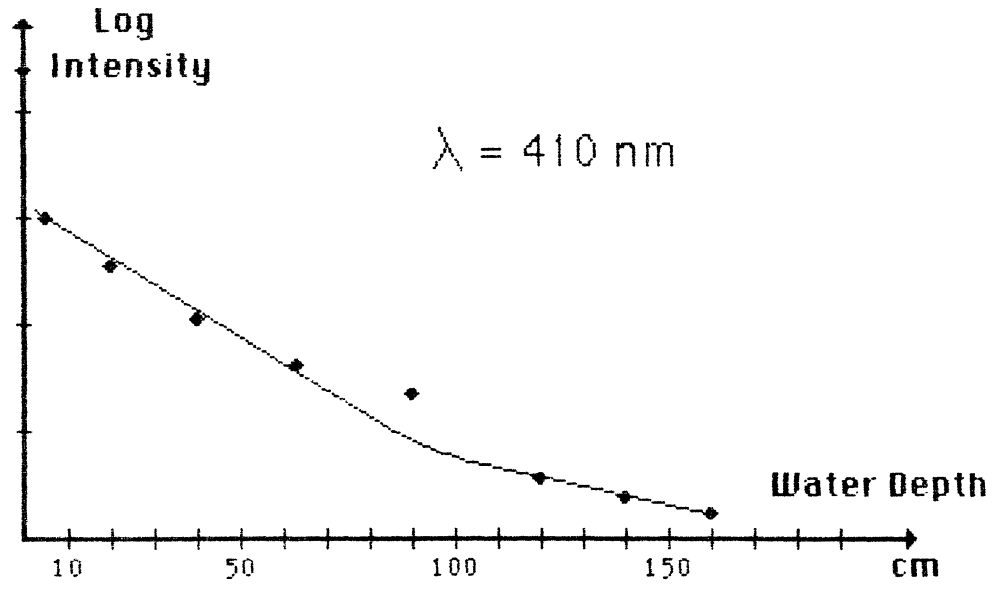

Fig. 15b. A logarithmic plot of the peak intensity values recorded in the same set-up as in Fig. 14.

However, in the present investigation different oils are primarily of interest, but the fluorescence intensities from oils were too weak to make a meaningful repetition for an oil of the just described experiment possible, at least with the equipment used. Despite of this, it is of interest to compare the integrated water fluorescence with the oil fluorescence spectra. A spectrum from water, 2 m deep, is in Fig. 16 compared with one from a crude oil. This figure shows that the fluorescence from water is almost comparable with the weakest oils in intensity, at least in the blue region of the spectrum. This fact can be worth noticing when chosing suitable wavelengths for distinguishing between oils.

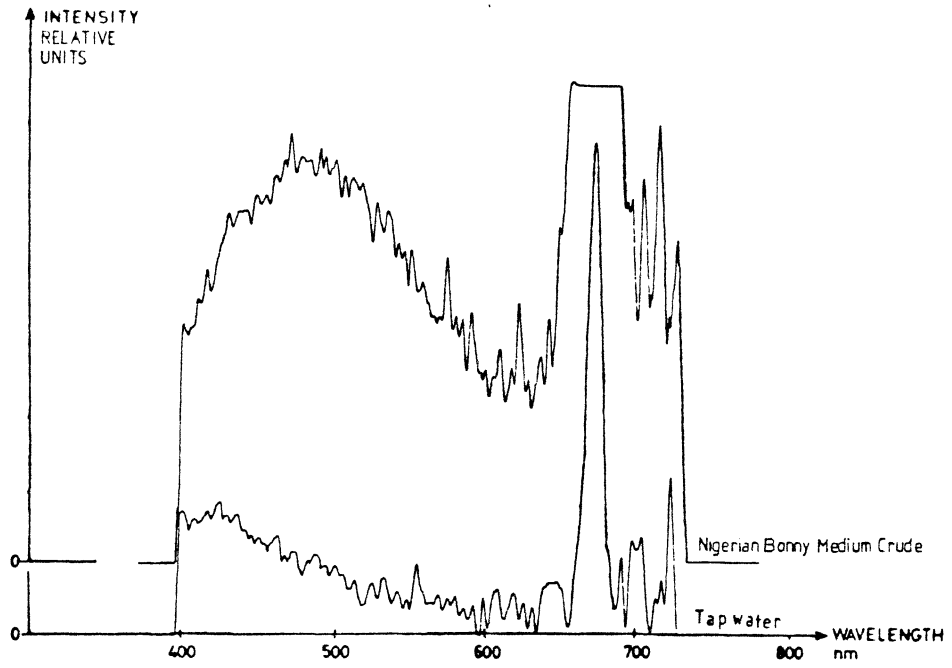

Fig. 16. Spectra of optically thick tap water (2m layer) and an optically thick crude oil.

A comparison for tap water and sea water is shown in Fig. 4b. The fluorescence of sea water as well as of tap water clearly varies a lot for different places and for different times. In all our measurements, however, sea water always had the weaker fluorescence.

The setup from Fig. 7 was used to detect oil on the bottom of the barrel and to do measurements with temporal resolution. The measurements with the plastic sheet was repeated, but now with a PMT as a detector. The experiment was also performed at night

time, when it was possible to have a maximum voltage on the PMT without drawing a too high background dc current. The oil exposed was the heavy fuel oil E 410 (Fig. 3a), enclosed in a fluorescence-free quartz bulb not to contaminate the barrel. (Oils are optically thick already at a few μm layer thickness [39].) The bulb was large enough to cover the whole beam diameter when it was placed in the barrel. Curves for the wavelengths 420 and 500 nm are shown in Figs. 17 and 18. The signal levels were small and no signal at all was significant at 600 nm even when the oil bulb was directly exposed without water. The sensitivity in the red region is very low for the PMT used (S-4 response). However, in order to try to explain the result for the two wavelengths used, one has to study both the oil and the water spectra in Fig. 3a and Fig. 4, respectively. The oil spectrum is broader and also shifted to the red compared to the water spectrum. At 420 nm the intensities do not differ much. One can measure the water intensity and the water plus oil intensity by moving the bulb outside and inside the laser beam, respectively. Since the fluorescence is about as strong for water as for oil, the measured intensity is expected to be about equal for all water depth. In an intermediate state with little water

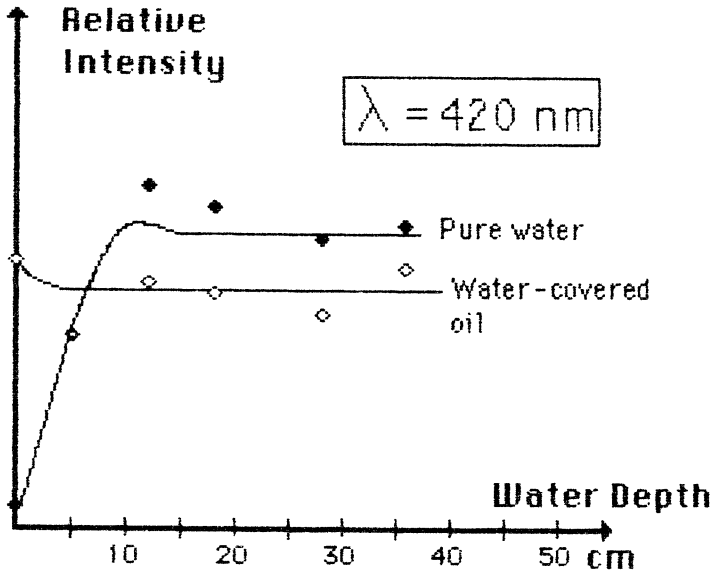

Fig. 17. Signal intensities from the PMT measurement on heavy fuel oil in water at 420 nm for different water depths.

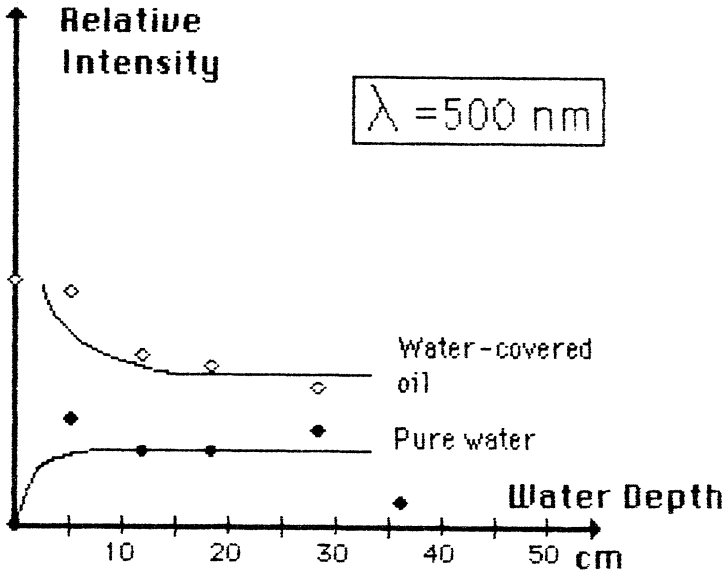

Fig. 18. Signal intensities from the PMT measurement on heavy fuel oil in water at 500 nm for different water depths.

fluorescence and more fluorescence from the oil the fluorescence intensity is greater in the lower part of the barrel than in the upper part, but it is then filtered by the water. Adding the intensities expressed by Eq. (2.3.1) and (2.3.2) gives that the fluorescence intensity from oil and water should be constant in this case in a first order approximation since $I_w(\infty) \approx I_{oil}(0)$. The actual measurement result can be seen in Fig. 17. To get an approximation of the oil signal the water fluorescence signal may be subtracted from the water plus oil fluorescence signal. In doing so an over-compensation is made since the barrel bottom reflectance is larger than the reflectance of the bulb. This affects the signal level to the depth at which the reflected laser intensity is negligible. For the fluorescence at 500 nm the situation is totally different. The oil fluorescence is here much stronger than the water fluorescence. The measured oil signal level should therefore approximately follow Beer-Lambert's law. The result of this experiment is that it is not possible to detect oil at a depth beyond 20 cm with the N_2-laser used.

The time-resolved measurements were performed to study how much the water surface state influenced the results. Both the elastically scattered light at 337 nm and the fluorescence light at 420 nm was included in this brief investigation. Examples of typical curves from the transient digitizer in the elastic case are shown in Fig. 19. It shows a prompt signal and an echo from the target. For the smooth surface the signal level from the target

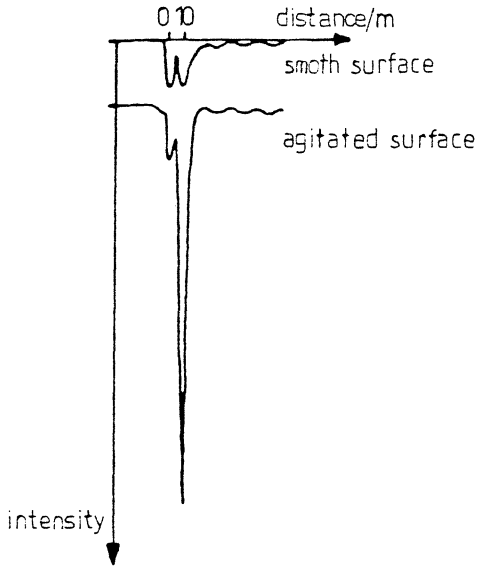

Fig. 19. Temporally resolved signals from the transient digitizer measuring the elastically scattered light at 337 nm. The curves are typical for what may happen if the laser beam is directly reflected into the telescope.

was very stable, but for the agitated water surface sometimes a huge signal from the specular reflection straight into the telescope turned up. A histogram showing this effect is presented in Fig. 20. For fluorescence light detection a corresponding influence could be caused by reflected sun light. This effect was, however, not measurable in our case. The fluorescence signal is very independent of the surface topology.

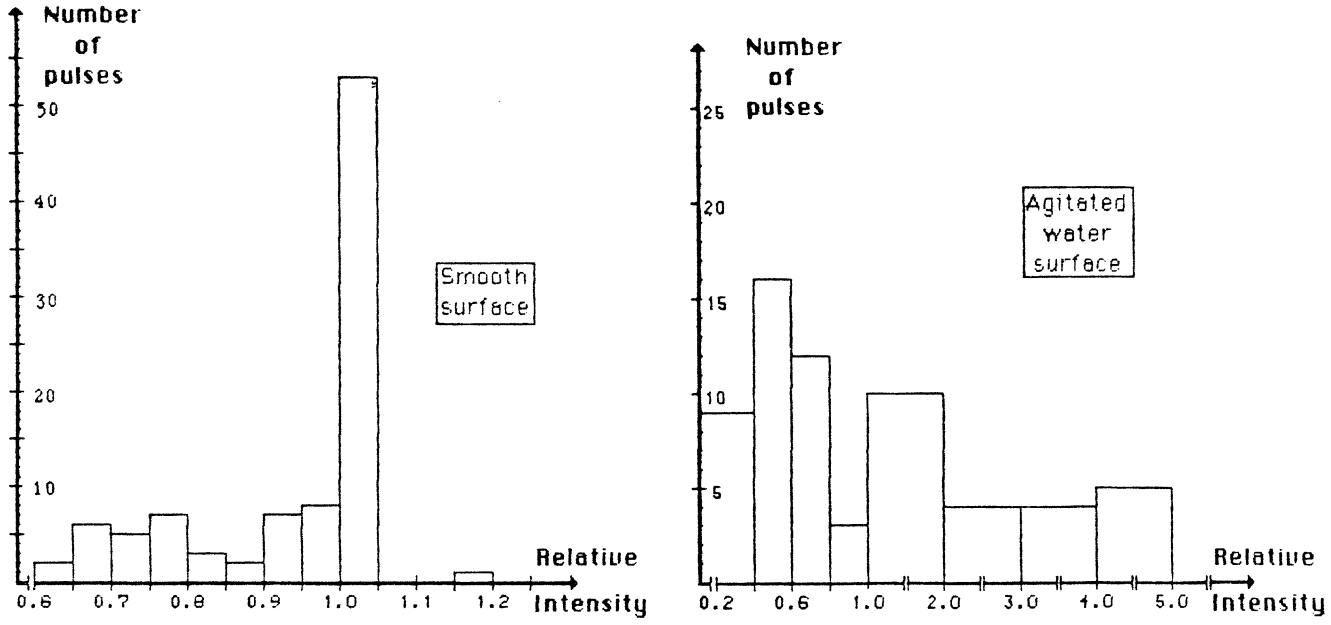

Fig. 20. Histograms for the ratios between target echo and start echo for the elastically scattered light at 337 nm.

3. Discussion

In order to distinguish between the three main oil types, detection in three wave-length bands is necessary as pointed out in Section 2.1. In an airborne system the intensities must be measured simultaneously. A problem may be that water might be confused with the refined products as seen in Table 1. Both the refined products and water will give A/B > 1 and B/C > 1. To avoid this confusion a fourth channel, D, detecting the water Raman peak at 384 nm can be used. A comparison between the 384 nm and the 410 nm signal (D/A) will eliminate such errors. Characterization of oil more than a few centimeters below the water surface will despite this be difficult since the water

fluorescence and the water filtering of the oil fluorescence changes the spectrum.

The competition with daylight is the most important limitation to the detection possibilities of an airborne system. The signal-to-background ratio is affected by the laser pulse energy, the target distance, the gate width (if gated integrators are used) and the quantum efficiency of the target approximately through the relation (compare (1.1) and (1.2))

$$S/B \sim \frac{P * q(\lambda)}{r^2 * \Delta t * \Omega * I_s(T)} \qquad (3.1)$$

where P is the laser power, $q(\lambda)$ is the target quantum efficiency at the actual wavelength, r is the target distance, Δt the gate width, Ω the telescope field of view and $I_s(T)$ the target surface radiance. The oil layer is assumed to be optically thick and the solid angle was kept constant in all our measurements. The telescope field of view must cover the spot illuminated by the laser beam which means that Ω is determined by the beam divergence. With the Quaker Ferrocoat 6828 oil, 70 m measuring distance and a gate time of 500 ns, 0.3 mJ of laser pulse energy was required at 420 nm to get a good S/B ratio in bright sunshine as seen in Fig. 11. The fluorescence intensity of a heavy fuel oil at 410 nm is about 30 times less than the intensity of the 6828 oil at 420 nm. That means that the distance has to be reduced a factor $(30)^{1/2}$ or the laser power increased with a factor 30 to get the same S/B ratio. On the other hand, if the gate width could be diminished e.g. to 50 ns, a factor 10 could be gained, that is a laser power of 0.9 mJ would do at 70 m distance. With the nitrogen laser used in the other measurements in Section 2.2 (with 100 µJ output energy per pulse) and a gate time of 500 ns, a target distance of maximum 8 m would be allowed in order to make a 410 nm detection of a heavy fuel oil possible. As seen in Table 1 this is the weakest intensity at the tabulated wavelengths among the oils investigated. It is not much stronger than the water fluorescence and it is therefore especially important in this case to know how the water influences the measurements, for instance with the use of the Raman peak. Some

Wave-length (nm)	Type of oil	Pulse energy (mJ)	Quantum effici-ency	Gate time (ns)	Tele-scope radii (cm)	Dis-tance (m)
	Daytime measurements					
410	Quaker Ferro-coat 6828	0.3	q_1	500	15	70
410	Heavy fuel oil	0.1	$q_1/30$	50	15	8
410	Heavy fuel oil	1.8	$q_1/30$	50	15	100
	Nighttime measurements					
600	Quaker ferro-coat 6828	0.1	$q_1/30$	500	25	30
410	Heavy fuel oil	1.8	$q_1/30$	50	25	300

Table 3: Examples of parameter combinations for an acceptable signal.

combinations of parameters for a LIF detection system is shown in Table 3.

The background changes will also cause problems. The addition of the background light to the signal will give an offset changing the ratios formed. The background can be measured separately, however, using the double-gate technique discussed in Section 4.

At night-time the I_s value is very low and thus it is not the background light but the electronic noise compared to the number of signal photons reaching the system that sets the detection limit. Here, a larger diameter telescope yields a better signal, which is not true at day-time. At day-time a larger telescope

collects more signal photons, but it also collects more background photons and thus does not increase the S/B ratio (for constant laser power) as seen in (3.1). During night-time the gate width has only a small influence. An approximate relation for the signal-to-noise ratio in this case would be (cp (1.1))

$$S/N \sim \frac{P * q * \Phi^2 * F(\lambda)}{r^2} \qquad (3.2)$$

where Φ is the telescope diameter and $F(\lambda)$ the spectral response of the detection system. Extrapolating from Fig. 9 a target distance of 30 m would be possible with a ϕ=25 cm telescope at night-time to detect a heavy fuel oil at 410 nm with a laser output of 100 μJ per pulse. It is less background light at night so PMT's can manage a higher voltage and are therefore more efficient detectors. However, all parameters but the telescope diameter are set for the day-time measurements. It should be desirable with a higher fligh ing altitude when it is dark. To be able to measure at 300 m height with the given parameters (1.8 mJ pulse energy) the telescope diameter needs to be 25 cm.

4. Construction Considerations

The different laser types that could be considered for an airborne system are listed in Table 4 together with some relevant properties. Excimer lasers have some chemical hazards and require special care. They also produce strong radio-frequency noise and their beam divergence is high. Copper vapour lasers have a very high repetition rate and low beam divergence. They need some maintenance, however, they need an hour warm-up time, they are heavy and the wavelength is not well suited for LIF. A small sealed-off nitrogen laser is light and easy to handle. Nitrogen lasers with larger pulse energy and higher repetition rates than 20 Hz are bigger and constructed for a continuos gas flow. They also produce rf-noise. All nitrogen lasers have a large beam divergence. A small tripled Nd:YAG laser seems to be the best alternative with its high energy and low beam divergence. The crystal mounting may require some maintenance when in an air-

technique.

Another factor that must be controlled is the changing background $I_s(T)$. If a background is superimposed on the signals it will of course affect the ratios A/B etc. The background level can be measured by opening the gate a second time without any fluorescence light present. This gate should be as close as possible to the gate that detects the signal so that the background does not change in the meanwhile. From Fig. 8 a-f we infer that this second gate must be at least 100 ns long. This signal could be used also as an input signal for regulating the high voltage to the PMT's in order not to saturate them.

A telescope size of ϕ = 25 cm should be enough. A mirror telescope may be preferrable to a lens telescope since a mirror telescope is achromatic.

Conclusion: A system using a laser as a light source should employ a tripled Nd:YAG laser or possibly a large nitrogen laser. The telescope should be a 25 cm diameter mirror telescope and the detection electronics gated integrators, the gate being trigged from the elastically scattered signal. Double-gate technique should be employed to avoid background influence and the characterization is best done by means of forming dimensionless ratios. It is probably most convenient to let the signal handling be done by a computer. Such a system should be capable of operational characterization of oil spills on or very close (dm) to the water surface. The prospects for detection and characterization of sunken oil with fluorescence techniques seem small.

The potential of flashlamps in air-borne fluorosensors should be investigated.

Acknowledgements

This work has been financed by the Swedish Space Corporation (SSC). We are grateful to civ. ing. Olle Fästh, project manager of the SSC, for fruitful discussions. The assistance by F.K. Eva Sjöholm is gratefully acknowledged.

REFERENCES

1. F. E. Hoge and R. N. Swift, "Experimental feasibility of the airborne measurement of absolute oil fluorescence spectral conversion efficiency", Appl. Opt. 22, 37 (1983)

2. L. A. Franks, G. A. Capelle and D. A. Jessup, "Aerial testing of an N_2 laser fluorosensor system", Appl. Opt. 22, 1717 (1983).

3 G. A. Capelle, L. A. Franks and D. A. Jessup, "Aerial testing of a KrF laser-based fluoresensor", Appl. Opt. 22, 3382 (1983).

4. F. E. Hoge, "Oil film thickness using airborne laser-induced oil fluorescence backscatter", Appl. Opt. 22, 3316 (1983).

5. W. F. Croswell, J. C. Fedors, F. E. Hoge, R. N. Swift and J. C. Johnson, "Ocean experiments and remotely sensed images of chemically dispersed oil spills", IEEE Transac. on Geosc. and Remote Sensing GE-21, 2 (1983).

6. J. F. Fantasia and H. C. Ingrao, "The development of an experimental airborne laser remote sensing system for the detection and classification of oil spills", in Proc. 9th Int. Conf. Remote Sensing Environ., Willow Run Labs., Environ. Res. Inst. Michigan (Ann Arbor, MI) Vol 3, 1711, April 15-19, 1974

7. J. F. Fantasia and H. C. Ingrao, "The development of an experimental airborne laser remote sensor for oil detection and classification in spills" U. S. Dept. Transportaton, Cambridge, MA, Final Rep. no. CG-D-86-75, 1975.

8. J. F. Fantasia, T. M. Hard and H. C. Ingrao, "An investigation of oil fluorescence as a technique for remote sensing of oil spills", U. S. Dept. Transportation, Cambridge, MA, Final Rep. DOT-TSC-USCG-71-7, 1974. .

9. R. Horvath, W. L. Margon and S. R. Stewart, "Optical remote sensing of oil slick: Signature analysis and system evaluation", Willow Run Labs., Inst. Sci. Tech., Univ. Michigan, Ann Arbor, MI, Proj. 724104.2/1, 1971.

10. R. T. V. Kung and I. Itzkan, "Absolute oil fluorescence conversion efficiency", Appl. Opt. 15, 409 (1975).

11. D. M. Rayner and A. G. Szabo, "Time-resolved laser fluorescensors: a laboratory study of their potential in remote characterization of oil", Appl. Opt. 17, 1624 (1978).

12. D. M. Rayner, M. Lee and A. G. Szabo, "Effect of sea-state on the performance of laser fluorescensors", Appl. Opt. 17, 2730 (1978).

13. H. Visser, "Teledetection of the thickness of oil films on polluted water based on the oil fluorescence properties", Appl. Opt. 18, 1746 (1979).

14. F. E. Hoge and R. N. Swift, "Oil film thickness measurement using airborne laser-induced water Raman backscatter", Appl. Opt. 19, 3269 (1980).

15 R. A. O'Neil, L. Buja-Bijunas and D. M. Rayner, "Field performance of a laser fluorosensor for the detection of oil spills", Appl. Opt. 19, 863 (1980).

16. Y. Pan, R. E. Faw and T. W. Lester, "Laser Raman remote temperature sensing in liquids", Exp. in Fluids 2, 81 (1984).

17. D. A. Leonard, B. Caputo and R. L. Johnson, "Experimental remote sensing of subsurface temperature in natural ocean water, Geophys. Res. Lett. 4, 279 (1977).

18. D. A. Leonard, B. Caputo and F. E. Hoge, "Remote sensing of subsurface water temperature by Raman scattering", Appl. Opt. 18, 1732 (1979).

19. W. M. Houghton, R. J. Exton and R. W. Gregory, "Field investigation of techniques for remote laser sensing of oceanographic parameters", Rem. Sens. Environ. 13, 17 (1983).

20. F. E. Hoge and R. N. Swift, "Airborne simultaneous spectroscopic detection of laser-induced water Raman backscatter and fluorescence from chlorophyll a and other naturally occurring pigments", Appl. Opt. 20, 3197 (1981).

21. H. H. Kim, "New Algae Mapping Technique by the Use of an Airborne Laser Fluorosensor", Appl. Opt. 12, 1454 (1973).

22. D. A. Leonard, B. Caputo and F. E. Hoge, "Remote sensing of subsurface water temperature by Raman scattering", Appl. Opt. 18, 1732 (1979).

23. F. E. Hoge and R. N. Swift, "Airborne dual laser excitation and mapping of phytoplankton photopigments in the Gulfstream warm core ring", Appl. Opt. 22, 2272 (1983).

24. E. V. Browell, "Analysis of laser fluoresensor systems for remote algae detection and quantification", NASA TN-D-8447, NASA Langley Res. Center, Hampton, Va. 1977.

25. G. D. Hickman and J. A. Edmonds, "Laser-induced marine bio-luminescence measurements and the potential for airborne remote sensing", Rem. Sens. Environ. 15, 77 (1984).

26. F. V. Bunkin, D. V. Vlasov, L. M. Gerasimenko and V. P. Slobodyanin, "Influence of temperature on the luminescence spectrum of blue-green algae", Sov. J. Quantum. Electron. 13, 1005 (1983).

27. F. E. Hoge and R. N. Swift, "Application of the NASA airborne oceanographic lidar to the mapping of chlorophyll and other organic pigments", NASA Conf. Publ. 2188, NOAA/NEMP III 81 ABCDFG 0042 (1981).

28. F. E. Hoge and R. N. Swift, "Delineation of estuarine fronts in the German Bight using airborne laser-induced water Raman backscatter and fluorescence of water column constituents", Int. J. Remote Sensing, Vol. 3, No. 4, 475-495, 1982.

29. O. Steinvall, H. Klevebrant, J. Lexander and A. Widen, "Laser depth sounding in the Baltic sea", Appl. Opt. 20, 3284 (1981).

30. F. E. Hoge, R. N. Swift and E. B. Frederick, "Water depth measurement using an airborne pulsed neon laser system", Appl. Opt. 19, 871 (1980).

31. G. D. Hickman and J. A. Edmonds, "Laser acoustic measurements for remotely determining bathymetry in shallow turbid waters", J. Acoust. Soc. Am. 73, 840 (1983).

32. D. A. Leonard and B. Caputo, "Raman remote sensing of the ocean mixed-layer depth", Opt. Eng. 22, 288 (1983).

33. F. E. Hoge and R. N. Swift, "Airborne detection of oceanic turbidity cells structure using depth-resolved water Raman backscatter", Appl. Opt. 22, 3778 (1983).

34. L. Celander, K. Fredriksson, B. Galle and S. Svanberg: Investigations of Laser-Induced Fluorescence with Applications to Remote Sensing of Environmental Parameters, Göteborg Institute of Physics Reports, GIPR-149 (1978).

35. B. Galle, T. Olsson and S. Svanberg, "The fluorescence properties of Jellyfish", Göteborg Institute of Physics Reports, GIPR-181 (1979). (In Swedish).

36. T. Olsson, "Possibilities of Sphagnum chartering by laser-induced fluorescence", unpublished report (in Swedish).

37. B. Galle, "Investigation of the possibility of detecting bulk-transported chemicals using remote sensing, based on laser-induced fluorescence", Göteborg Institute of Physics Reports, GIPR-220 (1980). (In Swedish).

38. S. Montán and S. Svanberg: A System for Industrial Surface Monitoring Utilizing Laser-Induced Fluorescence, to be published in Appl. Phys. B.

39. P. Herder, T. Olsson, E. Sjöblom and S. Svanberg, "Monitoring of Surface Layers Using Fluorescence Techniques", Lund Reports on Atomic Physics, LRAP-9 (1981).

40. K. Fredriksson, B. Galle, K. Nyström, S. Svanberg and B. Öström, "Underwater laser-radar experiments for bathymetry and fish-school detection", Göteborg Institute of Physics Reports, GIPR-162 (1978).

41. K. Fredriksson, B. Galle, K. Nyström, S. Svanberg and B. Öström, "Marine laser probing - Results from a field test", Medd. fr. Havsfiskelaboratoriet 245, (1979).

42. S. Montán, K. Svanberg and S. Svanberg, "Multicolor imaging and contrast enhancement in cancer-tumor localization using laser-induced fluorescence in hematoporphyrin-derivative-bearing tissue", Opt. Lett. 2, 56 (1985).